Synthesis, Structure, and Spectroelectrochemical Investigation of Novel Ternary Co/S(Se)/Sn Clusters Derived from Binary Cobalt Stannanediyl Complexes

Jörg J. Schneider,*[a] Jörg Hagen,[a] Dirk Spickermann,[a] Dieter Bläser,[a] Roland Boese,[a] Fabrizia F. de Biani,[b] Franco Laschi,[b] and Piero Zanello[b]

Dedicated to Prof. Dr. mult. Günther Wilke on the occasion of his 75th birthday

Abstract: The synthesis and structure of heterobimetallic Co/Sn complexes $[(\eta^5\text{-}Cp^R)Co{-}Sn\{CH(SiMe_3)_2\}_2]$ ($Cp^R = C_5Me_5$ **2**; C_5EtMe_4 **3**) are described. Insertion reactions of sulfur and selenium into the unbridged heteronuclear Co–Sn bonds of **1**, **2**, and **3** ($R = H_5$ **1**, Me_5 **2**, $EtMe_4$ **3**) have been studied. Depending on the stoichiometry of the chalcogen element used, novel ternary Sn–chalcogen–Co clusters (**8**, **9**, **15**, and **16**) can be synthesized, and their molecular structures, which represent rare examples of crystallographically characterized cases of ternary transition metal/chalcogen/tin complexes, have been determined. Electrochemistry shows that complexes **8** and **9** are able to support reversibly either the removal or addition of one electron. Insertion of a further (Cp)Co–E (E = chalcogen) fragment significantly affects the electron distribution and causes complexes **9** and **16** to undergo two consecutive one-electron oxidations. The EPR spectra of the respective monocations have been recorded. In all cases, the unpaired electron strongly interacts with the cobalt nucleus(i), thus testifying that the main contribution to the relevant HOMO orbitals comes from the cobalt atom(s).

Keywords: chalcogenides · cobalt · electrochemistry · stannanediyls · tin

Introduction

Metal–metal bonds M–M′ are frequently the weakest chemical bonds in multinuclear organometallics, and the clusters M_xL_n, therefore, represent the most reactive sites in these compounds. Oxidative addition reactions of bare elements or ER fragments (E = chalcogen, R = organic group) with metal–metal bonds in such compounds can occur either by conventional addition to a single metal atom of the M–M′ moiety, which is analogous to additions in mononuclear complexes, or by addition to the intact binuclear M–M′ site. The former leads to cleavage of the M–M′ bond, the latter to formation of a new [μ-ER(M–M′)] entity, in which the new ligand fragment ER or bare element E has added to the M–M′ bond, and is now bridging both metal fragments (Scheme 1a). In contrast, ER or E may insert into the M–M bond; this results in the formation of an ER or E bridge between M and M′, with the metal atoms no longer directly bonded to each other (Scheme 1b).

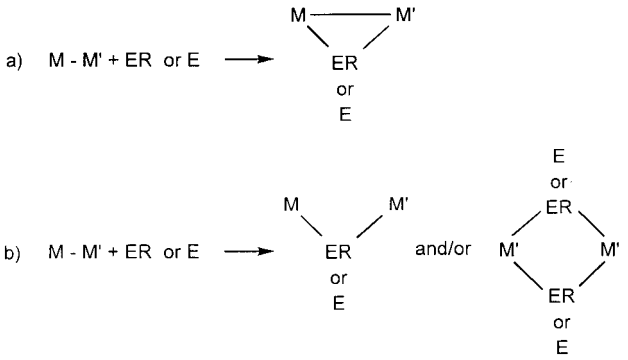

Scheme 1. Reaction scheme for the addition of E or ER with the metal–metal bond. M and M′ = different M_xL_y fragments.

Chalcogen elements, and organic or organometallic dichalcogenides with E–E linkages are very suitable candidates to explore these types of reactivity, since they exhibit a) a remarkable reactivity towards electrophiles, and b) a rich structural diversity (Scheme 2). This diversity has been extensively studied with respect to transition metal chalcogen carbonyl clusters.[1, 2] Oxidative additions of acyclic organic, cyclic organic, and organometallic dichalcogenides are also known.[3] Examples in which bare chalcogen elements insert

[a] Priv.-Doz. Dr. J. J. Schneider, Dr. J. Hagen, Dipl.-Chem. Dr. D. Spickermann, D. Bläser, Prof. Dr. R. Boese
Institut für Anorganische Chemie der Universität
Universitätsstraße 5–7, D-45117 Essen (Germany)
Fax: (+49) 208-183-4195
E-mail: joerg.schneider@uni-essen.de

[b] F. F. de Biani, Dr. F. Laschi, Prof. Dr. P. Zanello
Dipartimento di Chimica, via Aldo Moro
I-53100 Siena (Italy)

  0947-6539/00/0602-0237 $ 17.50+.50/0

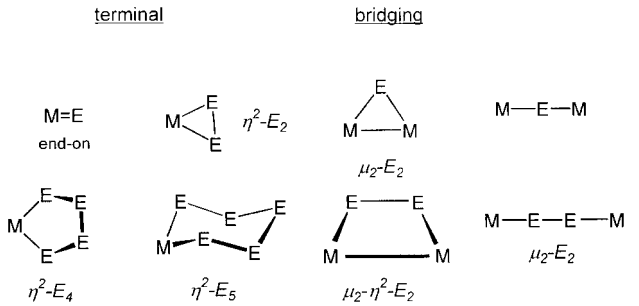

Scheme 2. Experimentally verified terminal and bridging coordination modes for chalcogen atoms and chalcogenide anions.

into M–M′ bonds that lead to M–E–M′ linkages, however, are still rare.[4] This holds true especially when M is a transition and M′ is a main group metal, and the fact that such reactions have been rarely observed may be attributed to a lack of synthetic methods that offer access to this type of compound. As a result of the multiple oxidation states of chalcogen atoms in such structures, they may promise a rich redox chemistry, are valuable candidates for the study of intramolecular electron transfer processes, and have the potential to act as molecular precursors for solid-state materials.[5]

Very recently we have described the synthesis, structure, and reactivity of $[(\eta^5\text{-}Cp^R)Co\text{–}Sn\{CH(SiMe_3)_2\}_2]$ (**1** $Cp^R = C_5H_5$), which is a unique complex with an unbridged Co–Sn bond and a subvalent threefold coordinated tin(II) atom.

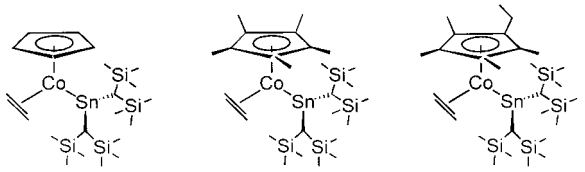

1[5] **2** **3**

Complex **1** adds elemental Se and Te to the Co–Sn bond, which leaves this bond intact (Scheme 1a) and thus allows access to the first heterotrinuclear Co/Sn/E complexes.[6]

Herein we report new experimental results in this field: a) synthesis and structural investigation of two new congeners of **1**, that is **2** ($Cp^R = C_5Me_5$), and **3** ($Cp^R = EtMe_4$), and b) novel reactivity of **1**, **2**, and **3** towards insertion of elemental sulfur and selenium into their Co–Sn bond. The new pentanuclear ternary complexes derived from these reactions are the first noncarbonyl containing Co/chalcogen/Sn complexes. They display diverse structures and a rich spectroelectrochemistry, which we have studied by X-ray crystallography, cyclic voltammetry, and macroelectrolysis coupled with EPR spectroscopy.

Results and Discussion

Synthesis of $[(\eta^5\text{-}Cp^R)Co\text{–}Sn\{CH(SiMe_3)_2\}_2]$ ($Cp^R = C_5Me_5$ 2, $Cp^R = C_5EtMe_4$ 3): The reflux of solutions of $[(\eta^5\text{-}Cp^R)(\eta^2\text{-ethene})_2Co]$ ($Cp^R = C_5Me_5$, **4**; $Cp^R = C_5Me_4Et$, **5**) in diethyl ether with Lappert's stannylene $[Sn\{CH(SiMe_3)_2\}_2]$ (**6**)[7] resulted in a color change of the initially brown-red solutions to purple and the evolution of ethene gas. Compounds **2** and **3** can be isolated, after work-up and crystallization from ether at $-78\,^\circ C$, as purple-black, very air-sensitive crystals, which are stable for a month even at room temperature and are best stored under ethene gas to preserve long-term stability (Scheme 3).

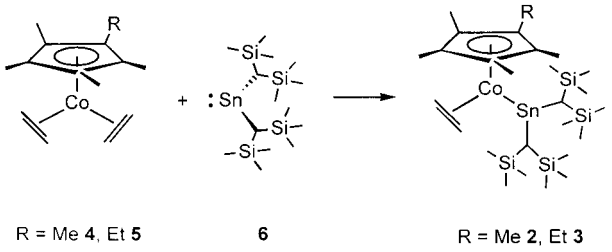

R = Me **4**, Et **5** **6** R = Me **2**, Et **3**

Scheme 3. Reaction scheme for the formation of **2** and **3**.

^1H and ^{13}C NMR data reveal that **1**,[6] **2**, and **3** are isostructural. As for **1**, all relevant proton signals for **2** and **3** are significantly shifted to higher field when compared with the bisethylene complexes **4** and **5**; this indicates the profound electronic influence of the $:SnR_2$ stannylene fragment on the 16 e $\{(\eta^5\text{-}Cp^R)Co(\eta^2\text{-ethene})\}$ fragments. The molecular structure of **2** was determined by X-ray crystallography (Figure 1).

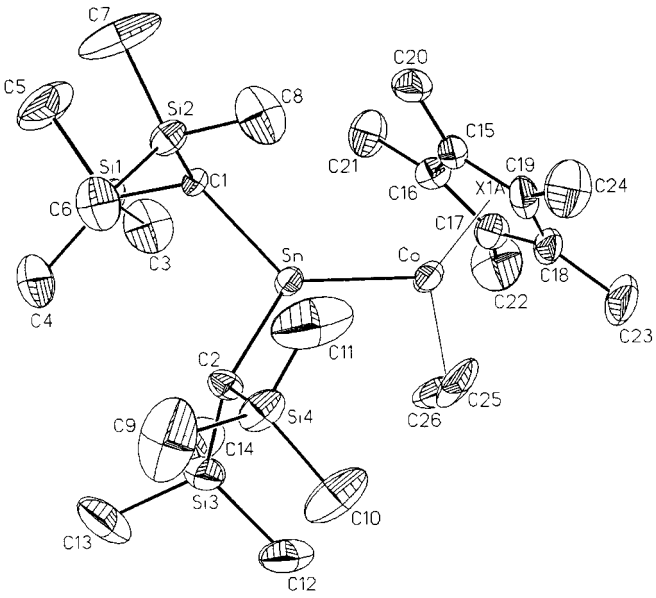

Figure 1. Molecular structure of **2** in the solid state. Selected bond lengths [Å] and angles [°] are: Sn–Co 2.386(2), Sn–C2 2.212(9), Sn–C1 2.239(8), Co–C26 1.95(2), C–C25 2.02(2), C2–Sn–C1 105.1(3), C2–Co–Sn 127.6(3), C1–Sn–Co 127.3(2).

Co and Sn are both trigonally planar coordinated. The short Co–Sn bond length is 2.386(2) Å and is in the same range as those determined for the Cp derivative **1**[6] and the bis(ethene)(stannylene)Ni complex $[(\eta^2\text{-}C_2H_4)_2Ni\text{–}Sn\{CH(SiMe_3)_2\}_2]$ (Ni–Sn, 2.38 Å). For this complex, strong Ni–Sn bonding with a significant extent of double bond contribution (Ni=Sn) is discussed merely on the basis of crystallographic and spectroscopic data.[8] Nevertheless it should be emphasized, that in these complexes the shortness of the M–Sn (Co,

0947-6539/00/0602-0238 $ 17.50+.50/0 *Chem. Eur. J.* **2000**, *6*, No. 2

Ni) bonds can be attributed to the fact that the tin is only threefold coordinated. In **1**–**3**, the stannylene [:Sn{CH(SiMe$_3$)$_2$}$_2$] fragment, which replaces ethene, serves as a two-electron donor, which thus results in a formal 18 valence electrons (VE) count on Co with the formation of a Co–Sn single bond. However, the short Co–Sn bond length might well be due to significant Co→Sn 5p$_\pi$ backbonding, but a more detailed discussion will require a theoretical investigation.

Inspection of a space-filling model of **2** after removal of the ethene ligand (Figure 2), discloses the Co–Sn bond as a preferential reaction site in this complex. Similar steric situations exist for **1**[6] and **3** after removal of the η^2-bonded ethene ligand.

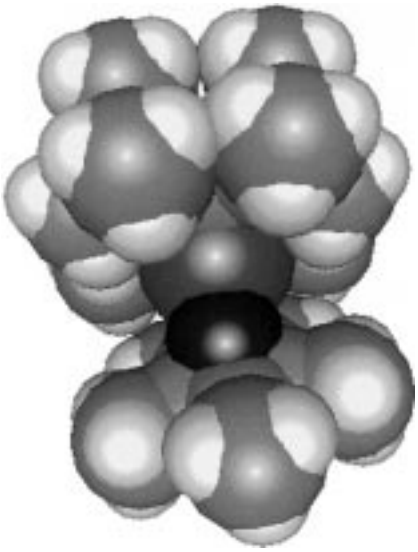

Figure 2. Space-filling model of **2** that shows the steric requirements of the ligand set and the steric situation for the unbridged Co–Sn bond in **2** after removal of the π-bonded ethene ligand.

After the removal of ethene from **1**–**3**, the Co–Sn bond of the remaining 16 e [(η^5-Cp^R)Co–Sn{CH(SiMe$_3$)$_2$}$_2$] fragments offers free access for incoming reaction partners. Consequently we have explored the reactivity of the heteronuclear Co–Sn bond of **1**–**3** towards insertion of elemental sulfur, selenium, and H_2S.

Reactivity of [(η^5-Cp^R)Co–Sn{CH(SiMe$_3$)$_2$}$_2$] (Cp^R = C$_5$Me$_5$ **2**, R = C$_5$EtMe$_4$ **3**) towards elemental sulfur and selenium

Synthesis of ***8***, ***9***, *and* ***10***: The addition of an equimolar amount of sulfur to a solution of **2** or **3** in diethyl ether at room temperature resulted in a color change from purple to red-brown within 10 min. It is noteworthy that all reactions can be performed as one-pot reactions, which start initially from the bis(ethene) complexes **4** and **5**. There is no need to isolate **2** or **3**, formed in situ, prior to reaction with sulfur. Final work-up of the crude reaction product by chromatography and fractional crystallization gave three different products (Scheme 4).

The binary complex **7** crystallizes as white, air-stable crystals and is also accessible by a direct reaction of Lappert's stannylene **6** with elemental sulfur.[9] Its spectral and analytical data are in full accord with those reported earlier by us.[9] These complexes are valuable single source precursors for the preparation of binary Sn/E films by MOCVD (metalorganic chemical vapor deposition) techniques.[10]

Compounds **8**, **9**, and **10** represent novel mixed ternary complexes derived from sulfur insertion into the Co–Sn bond, and all three complexes are thermally robust and give the corresponding molecular ions with the correct isotopic pattern in their mass spectra. The mixed ternary Co/S$_2$/Sn complex **8** is formed by a direct double insertion of sulfur into the Co–Sn bond of **2** after initial ethene loss has occurred. Regarding a possible formation pathway for **9** and **11** (see Scheme 5 for **11**), chalcogen insertion into the Co–Sn bond of **1**–**3** is evidently not the only route in the light of the observed stoichiometry of Co:S:Sn in **9** and **11**, which is 2:2:1. In addition to chalcogen insertion, partial fragmentation of **2** and **3**, and the redistribution of {(Cp)Co} fragments have to be considered. However, in contrast to the reaction of **2** with elemental sulfur, no formation of a ternary complex with Co$_2$/S$_2$/Sn stoichiometry was observed when **3** was treated with elemental sulfur.

Recently we have found that mixed metal complexes of the type [(η^5-Cp^R)M–Sn{CH(SiMe$_3$)$_2$}$_2$] (M = Fe, Co) are reactive towards H_2O.[11] As a result, we were able to synthesize the unsubstituted congener of **9**, **11** (Cp^R = C$_5$H$_5$), from the reaction of **1** with gaseous H_2S (Scheme 5). As found for the Me$_5$Cp derivative **9**, **11** is thermally robust and gives the molecular ion [**11**]$^+$ in the electron impact mass spectra at 140 °C and 70 eV.

Apart from **11** and as already observed for the reaction of **4** with S_8, the binary Sn/S compound **7** is also formed in this reaction (Scheme 5).

Synthesis of 13, **15**, **and 16**: The reaction of **1** with one equivalent of gray α-selenium proceeded within 12 h at room temperature (Scheme 6). During this time, the added selenium metal dissolved, and the color of the solution changed from purple to brown, which resulted in the formation of the

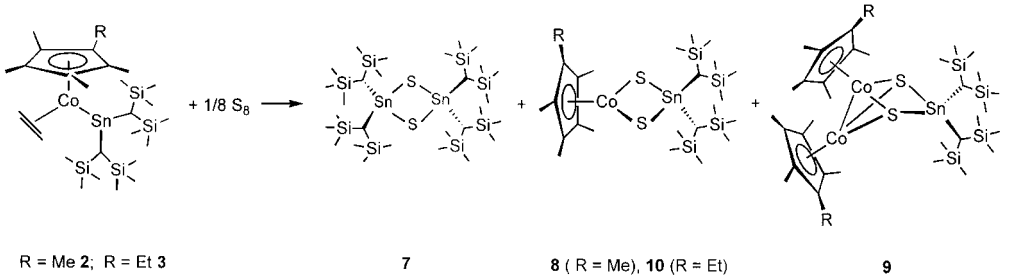

Scheme 4. Reaction scheme for the formation of **7**–**10**.

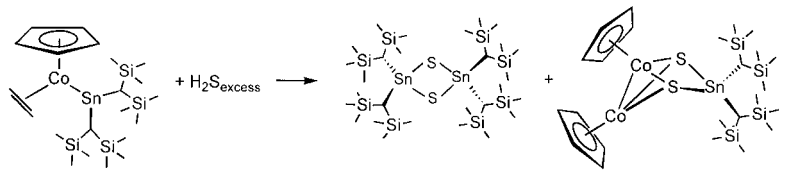

1 7 11

Scheme 5. Reaction scheme for the formation of **7** and **11** from **1**.

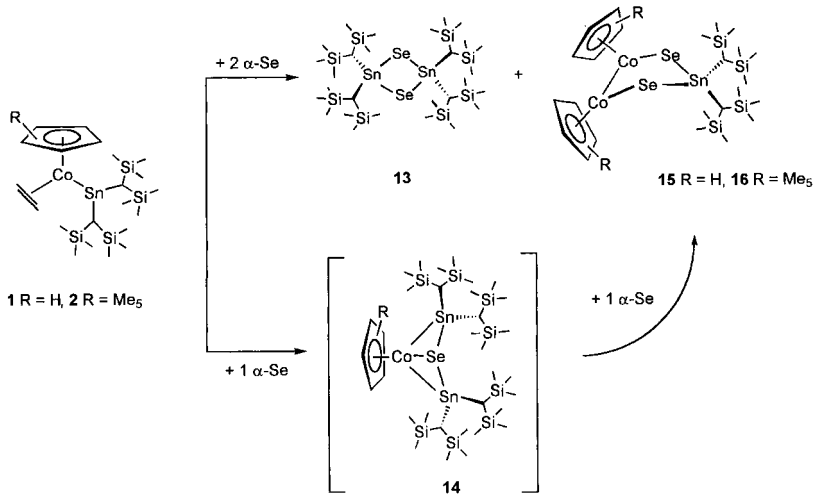

Scheme 6. Reaction scheme for the formation of **13**–**16**.

monoseleno complex **14**[6] as an intermediate. The addition of another equivalent of gray Se metal to this reaction mixture followed by stirring for 24 h caused this amount of Se metal to dissolve again. Subsequent work-up led to the isolation of the Se analogue of **7** (**13**), which had already precipitated as a white crystalline solid in pure form from the reaction solution. The main products, however, were the bis-seleno bridged complexes **15** (67%) and **16** (53%). As for the sulfur analogues **9** and **10**, the selenium congeners **15** and **16** are thermally very robust during the electron impact mass spectrometric measurements (70 eV, $T_{vap} = 150\,^{\circ}C$) and give $[M^+]$ signals with the correct isotopic pattern expected for the composition Co_2E_2Sn.

Thermogravimetric analysis (TGA) of **15** revealed four distinct regions of mass loss at 142, 197, 345, and 564 °C; this corresponds to a continous degradation of the cluster framework by ligand loss. This decomposition did not stop even at 600 °C, which indicates complex follow-up reactions of dissociated ligand molecules.[12] The ^1H and ^{13}C NMR spectra of all new complexes **8**–**11**, as well as **15**, are quite uncharacteristic with respect to a definite structure assignment. For example, for all complexes, only singlet resonances appear in their ^1H NMR spectra.

X-ray crystallographic studies of 8, 9, 15, and 16: Since the spectroscopic data set is definitely not distinctive enough with respect to an unambiguous structural characterization of the newly synthesized mixed Co/E/Sn clusters, single crystal structural investigations[13] were performed for **8**, **9**, **15**, and **16**. These investigations were carried out in order to elucidate their molecular structures unambiguously and to form a firm basis for further discussions about their spectroelectrochemical behavior. Experimental details are given in Table 1.

Molecular structure of 8: The molecular structure of the monocobalt cluster **8** is shown in Figure 3 and consists of a planar rectangle, in which the Co and Sn metal atoms are symmetrically bridged by two sulfur atoms.

The two sulfur atoms μ_2-bridge the Co and the tetrahedral Sn atom (C1–Sn–C2; 109.3(2) Å). The two sulfur atoms act as two-electron donors, which give Co a formal 16 VE count. The S–S bond length is 3.28 Å. This is well out of the range of E–E bond lengths found in tetrahedral transition metal clusters ($[Fe_2(\mu\text{-}E_2)(CO_6)]$[14]) of the bis-chalcogeno bridged *Hieber–Gruber*-type **A** (E = S, 2.86 Å;[15] E = Se, 2.293(2) Å[16]), in which E–E bonding of the bridging chalcogenes has been established in fundamental work by Dahl and co-workers.[15, 16] These short E–E bond lengths suggest a significantly enhanced nucleophilicity for the E–E bridge.[15–17]

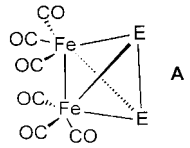

A

Owing to the long S–S atomic bond length in **8** relative to that in $[Fe_2(\mu\text{-}S_2)(CO_6)]$,[14] a lower basicity is expected, and hence a corresponding reactivity pattern as was observed for $[Fe_2(\mu\text{-}S_2)(CO_6)]$[16, 17] is not to be expected for **8**.

Molecular structures of 9, 15, and 16: Single-crystal investigations reveal that **9**, **15**, and **16** are isostructural. In all structures, the two Co atoms and the Sn atom form a triangle that is bridged by two capping μ_3-E atoms (Figure 4 and Figure 5). Presumably, from the steric strain, the Co–Co bond lengths in **9** and **16** are significantly elongated relative to those in **15**; this reflects the sterically encumbered situation imposed on the cluster geometry by the Me_5Cp (**16**, **9**) vs. Cp ligands (**15**).

The basal $\{(Cp)Co\}_2$ units contain a Co–Co bond while the apical SnR_2 fragment is tetrahedrally coordinated with two of these coordination sites occupied by bridging chalcogen atoms. In an alternative description according to Wade's

0947-6539/00/0602-0240 $ 17.50+.50/0 *Chem. Eur. J.* **2000**, *6*, No. 2

Table 1. Crystallographic data for **2**, **8**, **9**, **15**, and **16**.

	2	**8**	**9**	**15**	**16**
formula	$C_{26}H_{57}CoSi_4Sn \cdot Et_2O$	$C_{24}H_{53}CoS_2SnSi_4$	$C_{34}H_{68}Co_2S_2Si_4Sn$	$C_{24}H_{48}Co_2Se_2Si_4Sn$	$C_{34}H_{60}Co_2Se_2Si_4Sn$
M_w	677.71	695.76	889.91	843.45	999.71
crystal size [mm]	$0.34 \times 0.26 \times 0.19$	$0.42 \times 0.35 \times 0.27$	$0.47 \times 0.43 \times 0.13$	$0.41 \times 0.35 \times 0.27$	$0.43 \times 0.37 \times 0.29$
T [K]	298(2)	298(2)	298(2)	295(2)	295(2)
space group	$P2_1/n$	$P2_1/c$	$P\bar{1}$	$P2_1/c$	$P\bar{1}$
a [Å]	11.915(8)	8.9579(6)	11.7567(14)	16.9477(11)	11.5284(2)
b [Å]	20.716(5)	18.1885(13)	12.7987(13)	17.2519(11)	12.7126(2)
c [Å]	14.800(3)	23.0272(17)	17.3964(15)	12.1702(8)	17.9601(3)
α [°]	90	90	73.725(8)	90	90.5260(10)
β [°]	105.91(3)	99.559(2)	73.152(9)	95.8960(10)	106.2440(10)
γ [°]	90	90	63.064(7)	90	115.92(10)
V [Å^3]	3513(3)	3699.7(5)	2199.2(4)	3539.5(4)	2246.42(6)
Z (no. formula units)	4	4	2	4	2
ρ_{calcd} [g cm^{-3}]	1.281	1.249	1.344	1.583	1.478
collected reflections	6989	25787	5654	14507	8482
Θ_{max} [°]	25.00	25.71	22.53	25.66	25.73
unique reflections	5090	6519	5355	6054	6587
R_{merg} (all data)	0.029	0.041	0.041	0.0387	0.0709
observed reflections[a]	3420	5292	4190	5355	5922
parameters	298	280	370	316	371
μ [mm^{-1}]	1.34	1.38	1.53	3.83	3.03
min/max transmission	0.71/1.00[b]	0.74/1.00[b]	0.46/0.86[c]	0.0467/1.00[b]	0.20/0.80[d]
R_{merg} before/after corr.	0.0890/0.0216	0.0377/0.0256	0.0937/0.0473	0.1253/0.0266	0.1090/0.0663
$R1$ (obs. data)	0.0772	0.0466	0.0554	0.0500	0.0837
$wR2$ (all data)	0.2077	0.1258	0.1532	0.1281	0.2524
GOF (F^2, all data)	1.067	1.095	1.060	1.142	1.091
residual electron density [e Å^{-3}]	1.36	1.62	0.77	1.10	3.40
refinement comments	[e],[f]	[e],[f]	[e],[f]	[e],[f],[g]	[e],[f],[h]
diffractometer[i]	Siemens SMART[j]	Siemens SMART	Siemens P4	Siemens SMART	Siemens SMART

[a] Observation criterion $I > 2\sigma(I)$. [b] Empirical absorption correction based on equivalent reflections, Siemens-SADABS program. [c] Empirical absorption correction based on psi-scans, XEMP (Vers. 4.2) program in SHELXTL-package. [d] Empirical absorption correction based on equivalent reflections, Siemens-XEMP program. [e] SHELXTL (Vers. 5.03) progam package used for structure solving with Direct Methods and refinement on F^2. [f] Hydrogen atoms were calculated in ideal positions and treated as riding groups with the 1.2 fold (1.5 fold for methyl groups) value for the corresponding C atoms. [g] Cp rings were refined as rigid groups; C31 to C33 were disordered and refined with half occupancies. [h] Hydrogen atoms were calculated in ideal positions and treated as rigid groups, U values as for [f]; Cp rings as rigid groups. [i] Equipped with graphite monochromized $Mo_{K\alpha}$ radiation. [j] Detector distance 4.457 cm; the esds calculated by the program for the cell dimensions are probably too small and should be multiplied by a factor of 2–10.

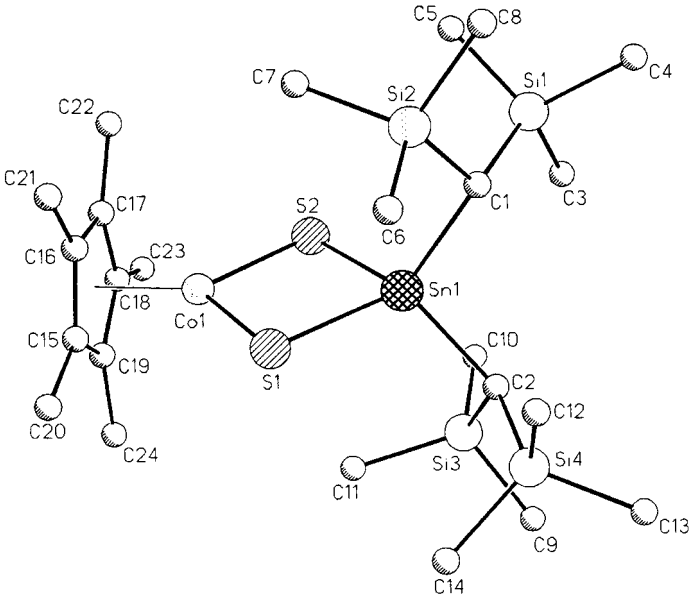

Figure 3. Molecular structure of **8** in the solid state. Selected bond lengths [Å] and angles [°] are: Sn1–S1 2.3904(12), Sn1–S2 2.3941(12), Co1–S1 2.1996(14), Co1–S2 2.1920(13), S–S 3.28, C1–Sn1–C2 109.3(2), Sn1–S1–Co1 88.29(4), Sn1–S2–Co1 88.498(4), S2–Sn1–S1 86.52(4), S2–Co1–S1 96.69(5).

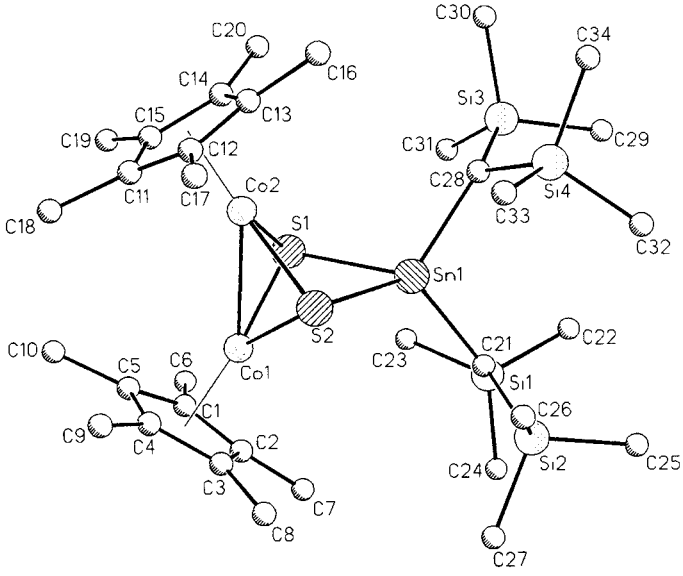

Figure 4. Molecular structure of **9** in the solid state. Selected bond lengths [Å] and angles [°] are: Sn1–S1 2.446(2), Sn1–S2 2.448(2), Co1–S1 2.230(2), Co1–S2 2.252(2), Co1–Co2 2.5162(14), Co2–S1 2.234(2), Co2–S2 2.238(2), S–S 3.05, Sn1–S1–Co1 86.91(7), Sn1–S2–Co1 86.37(6), Sn1–S1–Co2 86.53(7), Sn1–S2–Co2 86.49(7), Co1–S1–Co2 68.62(7), Co1–S2–Co2 68.17(7), S1–Co1–S2 85.91(8), S1–Co2–Se2 86.15(8), S1–Sn1–S2 77.21(7).

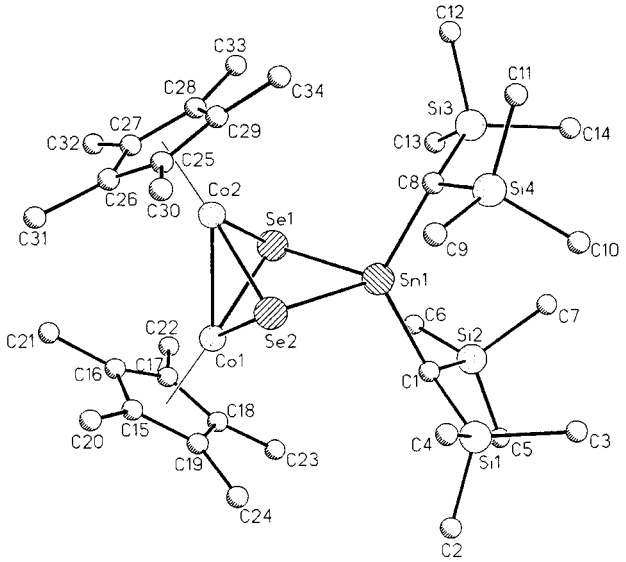

Figure 5. Molecular structure of **16** in the solid state. Selected bond lengths [Å] and angles [°] are: Sn1–Se1 2.5697(8), Sn1–Se2 2.555(2), Co1–Se1 2.3475(12), Co1–Se2 2.3554(12), Co1–Co2 2.4436(14), Co2–Se1 2.3494(12), Co2–Se2 2.3287(12), Se–Se 3.26, Sn1–Se1–Co1 83.21(30), Sn1–Se2–Co1 83.37(3), Sn1–S1–Co2 89.37(3), Sn1–Se2–Co2 89.37(3), Co1–Se1–Co2 58.69(4), Co1–Se2–Co2 58.02(3), Se1–Co1–Se2 88.02(4), Se1–Co2–Se2 88.61(4), Se1–Sn1–Se2 79.22(3). Selected bond lengths [Å] and angles [°] for **15** (without picture since it is isostructural to **16**) are: Sn1–Se1 2.5709(11), Sn1–Se2 2.5706(11), Co1–Se1 2.351(2), Co1–Se2 2.357(2), Co1–Co2 2.581(2), Co2–Se1 2.360(2), Co2–Se2 2.348(2), Se–Se 3.27, Sn1–Se1–Co1 85.77(4), Sn1–Se2–Co1 85.66(4), Sn1–S1–Co2 85.65(5), Sn1–Se2–Co2 85.88(4), Co1–Se1–Co2 56.62(5), Co1–Se2–Co2 56.58(5), Se1–Co1–Se2 87.53(5), Se1–Co2–Se2 87.52(5), Se1–Sn1–Se2 78.59(2).

terminology,[18] **9**, **15**, and **16** adopt a molecular structure based on a five-vertex, arachno cluster frame. Compounds **9**, **15**, and **16** belong to a group of mixed transition metal chalcogen arachno-type clusters, of which the transition metal/chalcogen complexes $[Fe_3(\mu_3Te)_2(CO)_9]$,[21] $[(Cp)_2Mo_2FeTe_2(CO)_7]$,[20] $[(CO)_6Fe_2Se_2Pt(PPh_3)_2]$,[17] and $[(CO)_6FeSe_2Pt(PPh_3)_2]$[17] represent structurally well characterized examples. However, well-characterized clusters in which chalcogen atoms bridge transition *and* main group metals are still scarce;[19] to the best of our knowledge, $[Tb(Tip)SnS_2Ru_2(CO)_6]$ and a series of $[Tb(Tip)SnS_{2,3}Os_{2,3}(CO)_{6,7}]$ complexes [Tip = 2,4,6-triisopropylphenyl; Tb = 2,4,6 tris{bis(trimethylsilyl)methyl}phenyl] are the only examples reported so far for the combination Sn/chalcogen/transition metal.[3]

Intracluster E–E bonding interactions should be considered for those clusters that contain more than one main group vertex.[20] The E–E bond lengths in **9**, **15**, and **16** are significantly shorter than the S–S bond length in the mononuclear Co derivative **8**. The S–S bond length of 3.28 Å in **8** contracts by 0.23 Å upon the formation of **9**. The short Se–Se bond lengths in **16** (3.27 Å) and **15** (3.26 Å) are in accord with this. It is likely that these reductions put significant strain on the Co_2Se_2Sn cluster framework of all three complexes. A possible reason for these short intramolecular E–E bond lengths is the steric constraints that are imposed by the fixed Co–Co bonds of the $\{(Cp^R)Co\}_2$ moieties. The strained Co–E–Co angles of 68.4° (E = S, MeCp), 58.35° (E = Se, Cp), and 56.60° (E = Se, Me_5Cp) in **9**, **15**, and **16**, respectively are in accord with this explanation. They compare well with the corresponding Fe–Te–Fe angles of 60° in $[(CO)_9Fe_3Te_2]$,[21] the Ru–S–Ru angles of 65.70° in $[Tb(Tip)SnS_2Ru_2(CO)_6]$,[3b] and the Mo–Te–Fe angles of 67.45° in $[Cp_2Mo_2FeTe_2]$,[20] which possess similar, constrained cluster frameworks. In addition, short Te–Te bond lengths have been reported for $[Cp_2Mo_2FeTe_2]$[20] (3.13 Å) and for $[(CO)_9Fe_3Te_2]$[21] (3.138 Å).

It is intriguing to look at the μ_2-E_2 fragments in the complexes **9**, **15**, and **16** as E_2 units bridging the dinuclear $\{(Cp)Co\}_2SnR_2$ metal core. Formation of these Co/Sn/E complexes can be understood in terms of the addition of subvalent (two electrons short of the usual group electron count) group 14 ER_2 fragments (E = Ge, Sn) to the μ-E_2 bridged transition metal fragments $\{(Cp)_2CoE_2\}$, which are electronically equivalent to the Hieber–Gruber-type clusters $[Fe(CO)_6E_2]$.[14] The analogy between our ternary clusters **9**–**11**, **15**, and **16** and clusters $[Fe(CO)_6M_2E_2]$ (E = S, Se, Te) is well established through the isoelectronic relationship between the 14 e (Cp)Co and the $Fe(CO)_3$ fragments. The addition of SnR_2 fragments to the E_2 chalcogen units of Hieber–Gruber-type clusters $[Fe(CO)_6E_2]$ by a photochemically induced addition of dimethylstannylene [:$SnMe_2$]—formed as a transient divalent fragment from $SnMe_6$—has been reported by Seyferth and co-workers.[4b, c] In these reactions, formation of isostructural mixed ternary transition metal/chalcogen/tin clusters related to **9**, **15**, and **16** was anticipated from their spectroscopic and analytical data. However, structural verification has been lacking so far.

Spectroelectrochemical studies on 8, 9, 10, and 16

Electrochemistry and coupled EPR measurements: The cyclic voltammetric response shows that complex **8** undergoes either an oxidation or a reduction process with features of chemical reversibility in dichloromethane (Figure 6).

Controlled potential coulometric tests performed on each one of the two redox steps proved that both the electrode processes involve one electron/molecule. Analysis of the

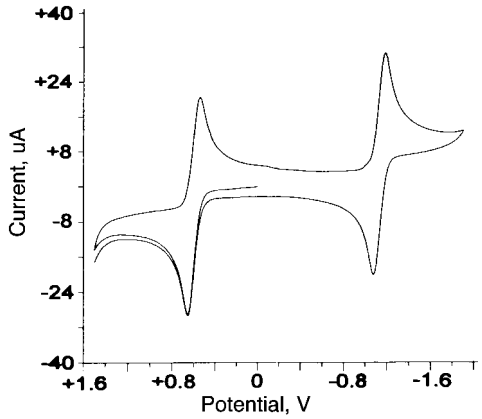

Figure 6. Cyclic voltammetric response recorded by using a platinum electrode in a solution of **8** (1.4×10^{-3} mol dm^{-3}) and $[NBu_4][PF_6]$ (0.2 mol dm^{-3}) in CH_2Cl_2. Scan rate 0.2 V s^{-1}.

0947-6539/00/0602-0242 $ 17.50+.50/0 *Chem. Eur. J.* **2000**, *6*, No. 2

cyclic voltammograms, with a scan rate that varies from 0.02 V s^{-1} to 5.12 V s^{-1}, suggests that the two redox processes are chemically and almost electrochemically reversible on the cyclic voltammetric timescale.[26] As a matter of fact, in both cases, the ratio $i_{p(backward)}/i_{p(forward)}$ is constantly equal to 1, and the current function $i_{p(forward)}/v^{1/2}$ remains essentially constant. As far as the peak-to-peak separation is concerned, it approaches the theoretical value of 60 mV (at least at low-scan rate) in the case of the cathodic step, whereas in the anodic step it departs somewhat from this value. This latter datum could be interpreted in the sense that the electron removal from **8** causes molecular strain that is somewhat greater than that caused by the electron addition.

The most significant electrochemical parameters of these redox changes are compiled in Table 2, together with those concerning the other complexes studied. In spite of this voltammetric picture, cyclic voltammetric tests performed on the solution that resulted from room-temperature, exhaustive one-electron oxidation ($E_w = +0.8$ V) proved the instability of the electrogenerated monocation $[\mathbf{8}]^+$ during the longer times of a macroelectrolysis experiment. Nevertheless, the paramagnetic $[\mathbf{8}]^+$ was revealed to be stable when the oxidation was performed at low temperature (−20 °C); this allowed us to record its EPR spectrum. Figure 7 shows the X-band spectrum recorded at 100 K.

Table 2. Electrochemical data for complexes **8**, **9**, **10**, and **16** in dichloromethane.

	$E_{0'}^{2+/+}$	ΔE_p^a	$E_{0'}^{+/0}$	ΔE_p^a	$E_{0'}^{0/-}$	ΔE_p^a
8			+0.60	98	−1.14	65
9			+0.64	66	−1.09	72
10	+0.58	80[b]	−0.44	64		
16	+0.58	77[b]	−0.42	68		

[a] Measured at 0.1 V s^{-1}. [b] Coupled to chemical complications.

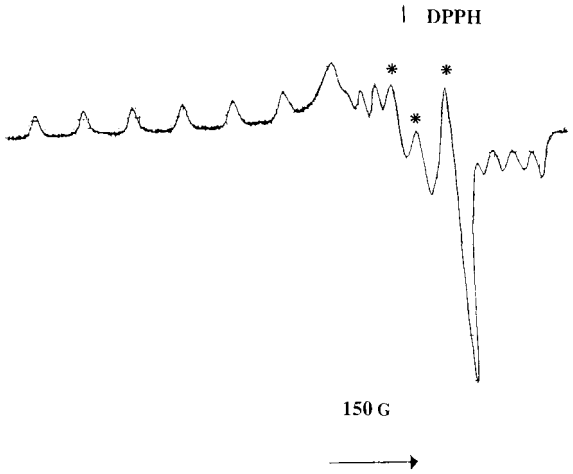

Figure 7. X-Band EPR spectrum recorded at 100 K for a solution of $[\mathbf{8}]^+$ in CH_2Cl_2 (see text).

The lineshape has a composite structure in that it exhibits two anisotropically structured S = ½ spectral multiplets that partially overlap. However, it must be noted that the sharp medium-field (starred) system is already present in the spectrum of the original (pre-electrolysis) solution of **8**. Such a metallic signal ($g_{\parallel} > g_{\perp} \approx g_{electron} = 2.0023$), which appears as a sharp doublet in the parallel region, but which lacks the corresponding resolution in the perpendicular region, is attributed to a paramagnetic tin species [I-Sn($^{115, 117, 119}$) = ½; natural abundance = 0.35, 7.6, and 8.6 %, respectively] that is likely to be present in the sample as an impurity.

Of even more interest is the widely extended absorption that displays well-separated anisotropic hyperfine octuplets with rhombic resolution [g_l, g_m, $g_h \approx g_{electron}$]. The absorption can be ascribed to the presence of a cobalt-centered paramagnetic species (I-Co^{59} = 7/2, 100 % natural abundance). The noticeable sharpness of such absorption and the lack of corresponding Sn and H nuclei couplings reflect the fact that the cobalt atom is the main contributor to the nature of the HOMO orbital. If the temperature is increased at the glassy-fluid transition, the anisotropic absorptions do not appear, and only the low-intensity isotropic signal of the tin-based radical species remains detectable ($g_{iso} = 2.022(5)$, $A_{iso} = 52(5)$ G; $T = 200$ K). Refreezing the fluid solution quantitatively restores the previous anisotropic pattern.

The same spectroelectrochemical behavior is exhibited by complex **10**. It is interesting to note that, although the HOMO–LUMO gap remains constant ($\Delta E^{0'} \approx 1.74$ V), the substitution of a methyl group for an ethyl group in the cyclopentadienyl ring makes the oxidation, unexpectedly, slightly more difficult and the reduction slightly easier. As far as the EPR spectrum of the monocation $[\mathbf{10}]^+$ is concerned, it almost parallels that of $[\mathbf{8}]^+$. Table 3 summarizes the relevant X-band EPR parameters.

Insertion of a further Cp–Co-chalcogen fragment into the cluster frame of **8** to obtain complex **10** causes important variations in the redox propensity. As Figure 8 shows, **10** undergoes two consecutive oxidation processes. A minor peak system is present in between the two steps, which is probably due to traces of some by-product.

Also in this case, the exhaustive oxidation at the first step ($E_w = -0.1$ V) consumes one electron per molecule and, when performed at low temperature, affords the stable monocation $[\mathbf{10}]^+$. In contrast, the second removal of an electron is complicated by chemical reactions that follow this electro-

Table 3. X-band EPR parameters of dichloromethane solutions of the monocations $[\mathbf{8}]^+$, $[\mathbf{9}]^+$, $[\mathbf{10}]^+$, and $[\mathbf{16}]^+$; $T = 100$ K. g values ± 0.006. A and ΔH values ± 5 Gauss.

	g_l	g_m	g_h	$\langle g \rangle$[a]	g_{iso}	A_l	A_m	A_h	$\langle A \rangle$[b]	A_{iso}	ΔH_{iso}
$[\mathbf{8}]^+$	2.285	2.058	1.986	2.110		83	23	32	46		
$[\mathbf{9}]^+$	2.288	2.067	1.983	2.113		90	28	37	48		
$[\mathbf{10}]^+$	2.332	2.126	1.956	2.138	2.126	28	44	30	34	≤ 7	95
$[\mathbf{16}]^+$	2.370	2.114	1.980	2.154	2.122	≤ 10	28	24	≤ 21	≤ 7	87

[a] $\langle g \rangle = (g_l + g_m + g_h)/3$. [b] $\langle A \rangle = (A_l + A_m + A_h)/3$.

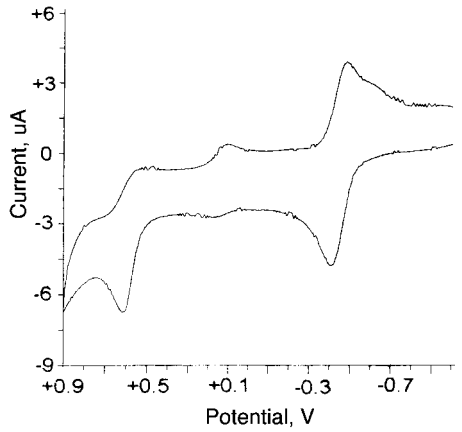

Figure 8. Cyclic voltammetric response recorded by using a platinum electrode in a solution of **10** (1.1×10^{-3} mol dm^{-3}) and $[NBu_4][PF_6]$ (0.2 mol dm^{-3}) in CH_2Cl_2. Scan rate 0.2 V s^{-1}.

chemical step, even when the experiment is carried out at low temperature. The substitution of the sulfur bridges for selenium bridges in **10** to obtain **16** produces no appreciable effect on the redox aptitude (Table 2).

The electrogenerated cation $[\mathbf{10}]^+$ gives rise, at 100 K, to a broad and poorly resolved spectrum, which becomes better resolved in the second derivative mode for the medium field (Figure 9a).

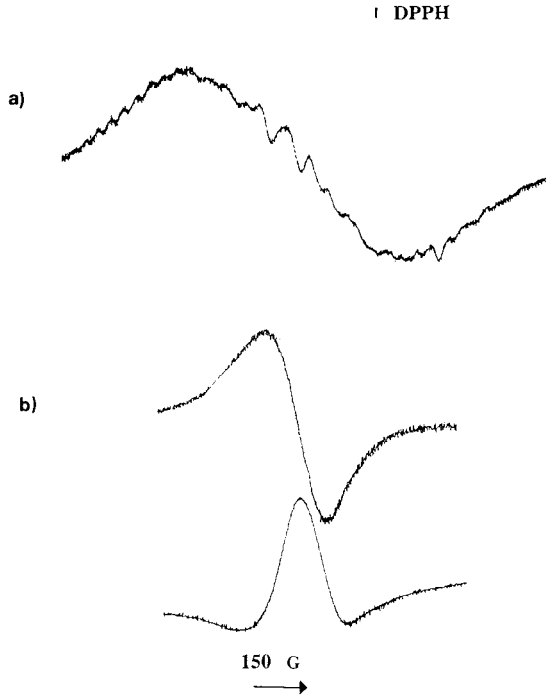

Figure 9. X-Band EPR spectra recorded for a solution of $[\mathbf{10}]^+$ in CH_2Cl_2. a) $T = 100$ K; b) $T = 298$ K.

The $S = ½$ hyperfine lineshape shows a rhombic structure ($g_i \neq g_{electron}$), the hyperfine (hpf) pattern of which is likely to arise from the magnetic interaction of the unpaired electron with two almost equivalent cobalt nuclei. This indicates that also in this case the HOMO orbital mainly consists of 3d Co atomic orbitals. An increase in the temperature at the glassy-fluid transition causes a consistent reduction of the spectral line width and the disappearance of the anisotropic hpf cobalt resolution, and at $T = 298$ K (Figure 9b) the signal becomes sharp and isotropic. The g_{iso} value fits the corresponding $\langle g \rangle$ well; this indicates that $[\mathbf{10}]^+$ essentially maintains its geometry under very different experimental conditions. Again, further refreezing quantitatively restores the original rhombic spectrum.

Quite similar spectral behavior is exhibited by the electrogenerated $[\mathbf{16}]^+$ monocation. The relevant EPR parameters are collected in Table 3.

Conclusion

We have presented the synthesis and structure of two new organobimetallic compounds (**2** and **3**), which have unbridged Co–Sn bonds and low-coordinate subvalent Sn^{II} atoms. We have shown that the insertion of bare chalcogen elements S and Se into the Co–Sn bond of **1**–**3** offers access to new ternary transition metal/chalcogen/tin clusters with a five-vertex, arachno cluster geometry, as determined by X-ray crystallography. We have pointed out that complexes **8**, **9**, **10**, and **16** display good redox propensity. In particular, the Co/S_2/Sn complexes **8** and **9** are able to add and remove one electron reversibly, whereas two subsequent electron removals occur in the Co_2/S_2 (or Se_2)/Sn complexes **9** and **16**. In all the relevant monocations, the unpaired electron essentially interacts with the cobalt nuclei. Apart from the rational insertion reaction of sulfur into the Co–Sn bond of **2** that leads to **8**–**11**, **15**, and **16**, formation of **11**, **15**, and **16** can be understood in terms of a formal addition of highly reactive, kinetically stabilized SnR_2 fragments to 16 e $\{(Cp^R)Co\}_2E_2$ fragments. We envisage access to a wider variety of ternary transition metal/chalcogen/main group metal clusters by adopting this idea for other ER_2 fragments (E = Ge, Sn, Pb) in future reactions.

Experimental Section

General: All reactions were carried out under an atmosphere of dry nitrogen gas with standard Schlenk techniques. Compounds **1**,[6] **4**,[24] **5**,[25] and **6**[7] were prepared according to published procedures. Microanalyses were performed by the microanalytical laboratory in the Chemistry Department of the University of Essen. Note: probably due to increased air sensitivity, elemental analysis of **3** was repeatedly below the typical analytical criteria for C–H combustion analysis of air-sensitive organometallic compounds (<1% in C). All solvents were dried according to standard procedures and were stored under nitrogen prior to use. The NMR spectra were recorded on a Bruker AC300 spectrometer (300 MHz for ^{1}H, 75 MHz for ^{13}C) and referenced against the remaining protons of the deuterated solvent. NMR samples were prepared by vacuum transfer of solvents onto the appropriate amount of solid sample, followed by flame-sealing of the NMR tube. MS spectra were recorded on a MAT8200 instrument under standard conditions (EI, 70 eV) and by using the fractional sublimation technique for the compound inlet. Material and apparatus for electrochemistry and coupled EPR measurements have been described elsewhere.[26] All the potential values are referred to the saturated calomel electrode (SCE). Under the present experimental conditions, the one-electron oxidation of ferrocene occurs at $E^{0'} = +0.38$ V. The external magnetic field H_0 for X-band ($\nu = 9.78$ GHz) EPR

0947-6539/00/0602-0244 $ 17.50+.50/0 Chem. Eur. J. 2000, 6, No. 2

measurements was calibrated by using a diphenylpicrylhydrazyl (DPPH) powder sample ($g_{DPPH} = 2.0036$).

Synthesis of [{(SiMe$_3$)$_2$CH}$_2$Sn–Co(η^5-Me$_5$Cp)(η^2-ethene)] (2) and [{(SiMe$_3$)$_2$CH}$_2$Sn–Co(η^5-EtMe$_4$Cp)(η^2-ethene)] (3): Solutions of **4** or **5** (3.6 mmol) in diethyl ether (100 mL) were stirred at room temperature for 12 h, whereupon the red-brown solutions turned intense purple, and gas evolution occurred. After heating these solutions under reflux for 12 h, no more gas evolution occurred. After filtration and recrystallization of the intense purple solutions, subsequent cooling to $-30\,^\circ$C and then to $-78\,^\circ$C afforded **2** and **3** as deep purple to black crystals (50 %), which were best stored below 0 °C under an ethene atmosphere to retain long-term stability (a month).

Compound **2**: IR (KBr): $\tilde{\nu} = 3050$, 1483, 1168 (η^2-ethene), 2947, 2901, 1402, 1246, 1012 (all SiMe$_3$), 2854, 1456, 1379, 1069, 1015, 842, 773, 755 cm^{-1} (all Me$_5$Cp); ^{1}H NMR ([D$_6$]benzene): $\delta = 2.46$ (br, $\nu_{1/2} = 20$ Hz, 2H; C$_2$H$_4$), 2.06 (br, $\nu_{1/2} = 23$ Hz, 2H; C$_2$H$_4$), 1.68 (s, 15H; Me$_5$Cp), 0.27 (s, 36H; SiMe$_3$), 0.05 (s, 2H; CH); ^{13}C NMR{^{1}H} ([D$_6$]benzene): $\delta = 90.21$ (s, 5C), 29.68 (s, C$_2$H$_4$), 11.07 (s, Me$_5$C$_5$), 4.67 (s, SiMe$_3$), 1.43 (s, CH); C$_{26}$H$_{57}$CoSi$_4$Sn (659.45): calcd C 47.30, H 8.71; found C 46.80, H 8.70.

Compound **3**: ^{1}H NMR([D$_6$]benzene): $\delta = 2.4$ (q, 2H; C*H*$_2$CH$_3$), 2.4 (2H; C$_2$H$_4$), 2.0 (2H; C$_2$H$_4$), 1.7 (s, 6H; CH$_3$), 1.6 (s, 6H; CH$_3$), 0.97 (t, 3H; CH$_2$C*H*$_3$), 0.28 (s, 36H); ^{13}C NMR{^{1}H} ([D$_6$]benzene): $\delta = 96.5$, 90.1, 89.4 (s, all EtMe$_4$*Cp*), 29.4 (C$_2$H$_4$), 20.3, 15.4 (both *Et*Me$_4$Cp), 10.8, 10.5 (both Et*Me*$_4$Cp), 4.5 (SiMe$_3$); C$_{27}$H$_{59}$CoSi$_4$Sn (673.74): calcd C 48.13, H 8.83; found C 46.80, H 9.01.

Synthesis of [{{(SiMe$_3$)$_2$CH}$_2$Sn}-μS$_2$–Co(η^5-Me$_5$Cp)] (8), [{{(SiMe$_3$)$_2$CH}$_2$Sn}-μS$_2$–{Co(η^5-Me$_5$Cp)}$_2$] (9), and [{{(SiMe$_3$)$_2$CH}$_2$Sn}-μS$_2$–Co(η^5-EtMe$_4$Cp)}] (10): Elemental sulfur (6.79 mmol) was added in one batch at room temperature to a solution of **2** or **3** prepared from **4** (6.79 mmol) and **5** (3.39 mmol) in diethyl ether (100 mL). After ten minutes, the color of the solution changed from purple to red-brown. The resulting solution was heated under reflux for 12 h, whereupon a white crystalline solid formed, in each case in moderate yields. The amount of this material was obviously dependent on the reflux time and increased for prolonged heating intervals; this indicates subsequent decomposition of product or possible side reactions. This material was isolated and characterized as **7**, and the identical spectral data were compared with those of the authentic material.[9] Chromatography (SiO$_2$, pentane, diethyl ether) gave trace amounts of **7**, as the first eluate, and then the main products **8** and **9**, as well-separated brown-red eluates. In the case of the reaction of **3** with sulfur, only trace amounts of the monocobalt complex **8**, as well as the main product **10** were isolated. Recrystallization of **8**, **9**, and **10** from diethyl ether afforded **8** (36 %), **9** (41 %), and **10** (30 %) as brown crystals. Single crystals of **8** and **9** suitable for X-ray analysis were obtained from diethyl ether/acetonitrile (2:1) at $-30\,^\circ$C.

Compound **8**: MS (EI, 70 eV, $T_{vap} = 95\,^\circ$C): *m*/*z* (%): 696 (30) [M^+], 537 (100) [$M^+ - $CH(SiMe$_3$)$_2$], 378 (20) [$M^+ - $ {CH(SiMe$_3$)$_2$}$_2$]; ^{1}H NMR ([D$_6$]benzene): $\delta = 1.42$ (s, 15H; CH$_3$), 0.34 (s, 36H; SiMe$_3$), -0.06 (s, 2H; CH); ^{13}C NMR{^{1}H} ([D$_6$]benzene): $\delta = 92.56$ (s, Me$_5$Cp), 14.21 (s, CH), 9.10 (s, CH$_3$), 4.02 (s, SiMe$_3$); C$_{24}$H$_{53}$CoS$_2$Si$_4$Sn (695.54): calcd C 41.41, H 7.68, S 9.21; found C 41.30, H 7.65, S 9.21.

Compound **9**: MS (EI, 70 eV, $T_{vap} = 155\,^\circ$C): *m*/*z* (%): 890 (5)[M^+] 571 (60), [$M^+ - $CH(SiMe$_3$)$_2$]; ^{1}H NMR ([D$_6$]benzene): $\delta = 1.92$ (s, 15H; CH$_3$), 1.88 (s, 15H; CH$_3$), 0.46 (s, 18H; SiMe$_3$), 0.39 (s, 18H; SiMe$_3$); ^{13}C NMR{^{1}H} ([D$_6$]benzene): $\delta = 85.00$ (s, Me$_5$Cp), 84.63 (s, Me$_5$Cp), 26.59 (s, CH), 26.26 (s, CH), 12.25 (s, CH$_3$), 12.08 (s, CH$_3$), 5.41 (s, SiMe$_3$), 5.05 (s, SiMe$_3$); C$_{34}$H$_{68}$Si$_4$SnCo$_2$S$_2$ (889.60): calcd C 45.78, H 7.71, S 7.21; found C 45.71, H 7.78, S 7.21.

Compound **10**: MS (EI, 70 eV, $T_{vap} = 155\,^\circ$C): *m*/*z* (%): 710 (23) [M^+], 551 (100) [$M^+ - $CH(SiMe$_3$)$_2$], 392 (3) [$M^+ - 2$CH(SiMe$_3$)$_2$]; ^{1}H NMR ([D$_6$]benzene): $\delta = 2.41$ (q, 2H; *CH*$_2$CH$_3$), 1.47 (s, 6H; Et*Me*$_4$Cp), 1.43 (s, 6H; Et*Me*$_4$Cp), 0.68 (t, 3H; CH$_2$*CH*$_3$), 0.35 (s, 36H; SiMe$_3$), -0.06 (s, 2H; *CH*(SiMe$_3$)); ^{13}C NMR{^{1}H} ([D$_6$]benzene): $\delta = 96.4$, 92.8, 91.7 (all Et-Me$_4$Cp), 18.0 (*C*H$_2$CH$_3$), 14.1 (*C*H(SiMe$_3$)), 12.9 (CH$_2$–*C*H$_3$), 9.1, 8.9, 3.9 (SiMe$_3$); C$_{25}$H$_{55}$CoS$_2$Si$_4$Sn (709.81): calcd C 42.30, H 7.81; found C 43.02, H 8.07.

Synthesis of [{{(SiMe$_3$)$_2$CH}$_2$Sn}-μSe$_2$–{Co{(η^5-Cp)}$_2$}] (15) and [{{(SiMe$_3$)$_2$CH}$_2$Sn}-μSe$_2$-{Co{(η^5-Me$_5$Cp)}$_2$}] (16): Elemental selenium (1.85 g, 1.13 mmol) was added in one batch at room temperature to a solution of **1** or **2** prepared from **4** (1.85 mmol - or 2.26 mmol of the Cp analogue of **4**) and **6** (0.93 g, 1.13 mmol) in diethyl ether (100 mL). After ten minutes, the color of the solution changed from purple to red-brown. In the case of **1**, Se (a second equivalent) was added after one hour of stirring, in which the first portion of selenium had already dissolved. The resulting clear, red-brown solutions were heated under reflux for 12 h, whereupon a white crystalline solid formed in both cases. This material was isolated and characterized as **13** by using its spectral data, which were identical to those of the authentic material.[9] The solvent was removed completely, and the residue was crystallized from diethyl ether or diethyl ether/acetonitrile mixtures. This resulted in shiny brown-black crystals of **15** (67 %) and **16** (53 %), which were stable in air for long periods of time. Single crystals suitable for X-ray analysis could be obtained from diethyl ether or diethyl ether/acetonitrile mixtures (2:1) at $-30\,^\circ$C.

Compound **15**: MS (EI, 70 eV, $T_{vap} = 140\,^\circ$C): *m*/*z* (%): 844 (30) [M^+], 685 (15) [$M^+ - $ {CH(SiMe$_3$)}], 626 (80) [$M^+ - $ Sn{CH(SiMe$_3$)$_2$}]; ^{1}H NMR ([D$_6$]benzene): $\delta = 4.85$ (s, Cp, 10H), 0.82 (s, CH, 2H), 0.36 (s, SiMe$_3$, 36H); ^{13}C NMR{^{1}H} ([D$_6$]benzene): $\delta = 75.6$ (s, ^2J(Sn,C) = 66.3 Hz, Cp), 23.6 (s, CH), 4.48 (s, ^3J(Sn,C) = 18.3 Hz, ^1J(Si,C) = 50.8 Hz, SiMe$_3$); C$_{24}$H$_{48}$Co$_2$Se$_2$Si$_4$Sn (843.22): calcd C 34.13, H 5.73; found C 34.29, H 6.03.

Compound **16**: MS (EI, 70 eV, $T_{vap} = 150\,^\circ$C): *m*/*z* (%): 984 (15) [M^+] 666 (50) [$M^+ - $ {CH(SiMe$_3$)$_2$}$_2$], 548 (20) [$M^+ - $ Sn{CH(SiMe$_3$)$_2$}$_2$]; ^{1}H NMR ([D$_6$]benzene): $\delta = 2.02$ (s, 15H), 2.01 (s, 15H), 1.66 (s, 2H), 0.51 (s, 18H), 0.50 (s, 18H); ^{13}C NMR{^{1}H} ([D$_6$]benzene): $\delta = 83.46$ (s, Me$_5$Cp), 23.68 (s, CH), 12.32 (s, CH$_3$), 4.75 (s, TMS); C$_{34}$H$_{68}$Co$_2$Se$_2$Si$_4$Sn (983.39): calcd C 41.49, H 6.92; found C 41.08, H 7.01.

Reaction of [{(SiMe$_3$)$_2$CH}$_2$Sn–Co(η^5-Cp)(η^2-ethene)] (1) with H$_2$S. Synthesis of [{{(SiMe$_3$)$_2$CH}$_2$Sn}-μS$_2$–{Co(η^5-Cp)(η^2-ethene)}$_2$] (11): A Schlenk tube containing a solution of **1** in diethyl ether (100 mL) was evacuated to 100 mbar, and dry N$_2$ saturated with H$_2$S was allowed in until ambient pressure was reached. Immediately after gas was allowed in, the color changed from purple to brown. After 10 min of stirring, the solvent was removed in a vacuum, and the solid residue was dissolved in diethyl ether and filtered. Crystallization at $-30\,^\circ$C gave white crystals of **7** as a first crop (0.34 mmol), which were isolated by decanting the supernatant. Addition of acetonitrile and subsequent cooling of the solution to $-30\,^\circ$C afforded brownish-red crystals of **11** (0.83 mmol).

Compound **11**: MS (EI, 70 eV, $T_{vap} = 140\,^\circ$C): *m*/*z* (%): 750 (70) [M^+], 591 (30) [$M^+ - $CH(SiMe$_3$)$_2$], 432 (100) [$M^+ - $ {CH(SiMe$_3$)$_2$}$_2$]; IR (KBr): $\tilde{\nu} =$ 2948, 2894, 2843, 1403, 1249, 1025, 981, 808, 662 (all Si(CH$_3$)$_3$), 3096, 1343, 1299, 1107, 1009, 841 cm^{-1} (all Cp); ^{1}H NMR ([D$_6$]benzene): $\delta = 5.03$ (s, 10H; Cp), 0.47 (s, 36H; SiMe$_3$), 0.66 (s, 2H; CH); ^{13}C NMR{^{1}H} ([D$_6$]benzene): $\delta = 76.91$ (s, 10C; Cp), 40.93 (s, 2C; CH), 4.30 (s, 12C; SiMe$_3$); C$_{24}$H$_{48}$Co$_2$S$_2$Si$_4$Sn (749.43): calcd C 38.43, H 6.47; found C 38.50, H 6.63.

Acknowledgments

This work was supported by the DFG (Heisenberg fellowship to J.J.S. and Sachbeihilfe grant SCHN 375/3-1), the Fonds der Chemischen Industrie, and the Volkswagen Foundation. We thank Dr. D. Stöckigt and Dr. K. Seevogel and co-workers (MPI für Kohlenforschung, Mülheim) for recording MS and IR spectra. P.Z. gratefully acknowledges the financial support of MURST of Italy (quota 40 %-1998).

[1] H. Vahrenkamp, *Angew. Chem.* **1975**, *87*, 363; *Angew. Chem. Int. Ed. Engl.* **1975**, *14*, 322.

[2] R. G. Hayter, F. S. Humiec, *J. Inorg. Nucl. Chem.* **1964**, *26*, 807; R. Zanella, R. Ros, M. Graziani, *Inorg. Chem.* **1973**, *12*, 2737; C. T. Lam, C. V. Senoff, *Can. J. Chem.* **1972**, *50*, 1868; S. J. Markham, Y. L. Chung, G. D. Branum, D. M. Blake, *J. Organomet. Chem.* **1976**, *107*, 121; M. H. J. M. de Croon, H. L. M. van Gaal, A. Van der Ent, *Inorg. Nucl. Chem. Lett.* **1974**, *10*, 1081; R. B. King, *Inorg. Chem.* **1963**, *2*, 641; A. Davison, N. Edelstein, R. H. Holm, A. H. Maki, *Inorg. Chem.* **1964**, *3*, 817; B. K. Teo, F. Wudl, J. H. Marshall, A. Kruger, *J. Am. Chem. Soc.* **1977**, *99*, 2349; A. W. Gal, J. W. Gosselink, F. A. Vollenbroek, *Inorg. Chim. Acta*, **1975**, *32*, 235; B. K. Teo, P. A. Snyder-Robinson, *Inorg. Chem.* **1987**, *17*, 3489; B. K. Teo, P. A. Snyder-Robinson, *J. Chem. Soc.*

Chem. Commun. **1979**, 255; D. Seyferth, R. S. Henderson, L. C. Song, G. B. Womack, *J. Organomet. Chem.* **1985**, *192*, 9; D. Seyferth, R. S. Henderson, L.-C. Song, *Organometallics* **1982**, *1*, 125; R. B. King, P. M. Treichel, F. G. A. Stone, *J. Am. Chem. Soc.* **1961**, *83*, 3600; R. B. King, M. B. Bisnette, *Inorg. Chem.* **1965**, *4*, 482; R. G. Hayter, F. S. Humiec, *J. Inorg. Nucl. Chem.* **1964**, *26*, 807; R. Zanella, R. Ros, M. Graziani, *Inorg. Chem.* **1974**, *12*, 2737; C. T. Lam, C. V. Senoff, *Can. J. Chem.* **1972**, *50*, 1868; Y. L. Markham, G. D. Chung, G. D. Branum, D. M. Blake, *J. Organomet. Chem.* **1976**, *107*, 121; M. H. J. M. de Croon, H. L. M. van Gaal, A. van der Ent, *Inorg. Nucl. Chem. Lett.* **1974**, *10*, 1081; G. Fachinetti, C. Floriani, *J. Chem. Soc. Dalton Trans.* **1974**, 2433; J. Werner, B. Juthani, *Z. Anorg. Allg. Chem.* **1981**, *473*, 107; R. B. King, *Inorg. Chem.* **1963**, *2*, 641; A. Davison, N. Edelstein, R. H. Holm, A. H. Maki, *Inorg. Chem.* **1963**, *2*, 817; B. K. Teo, F. Wudl, J. H. Marshall, A. Krueger, *J. Am. Chem. Soc.* **1977**, *99*, 2349; A. W. Gaal, J. W. Gosselink, F. A. Vollenbroek, *Inorg. Chim. Acta* **1979**, *32*, 235; B. K. Teo, P. A. Snyder-Robinson, *Inorg. Chem.* **1978**, *17*, 3489; B. K. Teo, P. A. Snyder-Robinson, *J. Chem. Soc. Chem. Commun.* **1979**, *255*; V. N. Drozd, V. I. Sokolov, V. V. Serggeichuk, *Izv. Akad. Nauk. SSSR. Ser. Khim.* **1981**, 1624; B. K. Teo, P. A. Snyder-Robinson, *Inorg. Chem.* **1981**, *20*, 4235; S. A. Khattab, L. Marko, G. Bor, B. Marko, *J. Organomet. Chem.* **1964**, *1*, 373; M. Cowie, R. L. DeKock, T. R. Wagenmaker, D. Seyferth, R. S. Henderson, M. K. Gallagher, *Organometallics* **1989**, *8*, 119; W. Eikens, P. G. Jones, C. Kienitz, C. Thöne, *J. Chem. Soc. Dalton Trans.* **1994**, 3329; W. Eikens, S. Jäger, P. G. Jones, C. Thöne, *J. Organomet. Chem.* **1996**, *511*, 67; W. Eikens, S. Jäger, P. G. Jones, J. Laube, C. Thöne, *Chem. Ber.* **1996**, *129*, 1275; P. G. Jones, J. Laube, C. Thöne, *Inorg. Chem.* **1997**, *36*, 2097; P. G. Jones, J. Laube, C. Thöne, *Acta. Crystallogr. Sect. C* **1997**, *53*, 1539; W. Eikens, P. G. Jones, C. Thöne, *Z. Anorg. Allg. Chem.* **1997**, *623*, 735; S. Jäger, P. G. Jones, J. Laube, C. Thöne, *Z. Anorg. Allg. Chem.* **1999**, *625*, 352.

[3] a) N. Tokitoh, Y. Matsuhashi, R. Okazaki, *Organometallics*, **1993**, *12*, 2894; b) Y. Matsuhashi, N. Tokitoh, R. Okazaki, *Organometallics*, **1994**, *13*, 4387; c) K. Merzweiler, L. Weise, *Z. Naturforsch. B* **1990**, *45*, 971; e) K. Merzweiler, H. Kraus, L. Weise, *Z. Naturforsch. B* **1993**, *48*, 287; d) K. Merzweiler, H. Kraus, *Z. Naturforsch. B* **1997**, *52*, 635.

[4] a) R. D. Adams, D. A. Katahira, *Organometallics* **1982**, *1*, 460; b) D. Seyferth, R. S. Henderson, M. K. Gallagher, *J. Organomet. Chem.* **1980**, *193*, C75; c) D. Seyferth, R. S. Henderson, *J. Organomet. Chem.* **1981**, *204*, 333; d) C. J. Cardin, D. J. Cardin, J. M. Power, *J. Am. Chem. Soc.* **1985**, *107*, 505; e) N. Viswanathan, E. D. Morrisson, G. L. Geoffroy, S. J. Grib, A. L. Rheingold, *Inorg. Chem.* **1986**, *25*, 3100.

[5] a) M. A. Ansari, J. A. Ibers, *Coord. Chem.* **1990**, *100*, 223; b) D. Coucouvanis, *Acc. Chem. Res.* **1991**, *24*, 1; c) L. C. Roof, J. W. Kolis, *Chem. Rev.* **1993**, *93*, 1037; d) M. G. Kanatzidis, S. P. Huang, *Coord. Chem. Rev.* **1994**, *130*, 509; e) J. Arnold, *Prog. Inorg. Chem.* **1995**, *43*, 353.

[6] J. J. Schneider, J. Hagen, D. Bläser, R. Boese, *Angew. Chem.* **1997**, *109*, 771; *Angew. Chem. Int. Ed. Engl.* **1997**, *36*, 739.

[7] a) D. E. Goldberg, D. H. Harris, M. F. Lappert, K. M. Thomas, *J. Chem. Soc. Chem. Commun.* **1976**, 261; b) For a recent review dealing with **6**, as well as other SnR_2 heavier element carbene homologues, see: P. P. Power, *J. Chem. Soc. Dalton Trans.* **1998**, 2939.

[8] C. Pluta, K. R. Pörschke, R. Mynott, P. Betz, C. Krüger, *Chem. Ber.* **1991**, *124*, 1321.

[9] J. J. Schneider, J. Hagen, O. Heinemann, J. Bruckmann, C. Krüger, *Thin Solid Films* **1997**, *304*, 144.

[10] K. H. Dahmen, I. S. Chuprakov, J. J. Schneider, J. Hagen, *Chem. Mater.* **1998**, *10*, 3467.

[11] J. J. Schneider, J. Hagen, J. Ensling, P. Gütlich, S. R. Mason, R. Bau, C. Krüger, *Chem. Eur. J.* **2000**, *6*, in press.

[12] K. H. Dahmen, I. S. Chuprakov, unpublished results, Florida-State University, **1997**.

[13] X-ray analysis of **2**, **8**, **9**, **15**, and **16**: Crystallographic data (excluding structure factors) for the structures reported in this paper have been deposited with the Cambridge Crystallographic Data Centre as supplementary publication nos. CCDC-113869 (**2**), 113871 (**8**), 113870 (**9**), 113872 (**15**), and 113873 (**16**). Copies of the data can be obtained free of charge on application to CCDC, 12 Union Road, Cambridge CB2 1EZ, UK (fax: (+44) 1223-336-033, e-mail: deposit @CCDC.cam.ac.uk).

[14] a) W. Hieber, J. Gruber, *Z. Anorg. Allg. Chem.* **1958**, *296*, 91; b) W. Hieber, W. Beck, *Z. Anorg. Allg. Chem.* **1963**, *2*, 328.

[15] C. H. Wei, L. F. Dahl, *Inorg. Chem.* **1965**, *4*, 1.

[16] C. F. Campana, F. Y.-K. Lo, L. F. Dahl, *Inorg. Chem.* **1979**, *18*, 3060.

[17] D. A. Lesch, T. B. Rauchfuss, *Inorg. Chem.* **1981**, *20*, 3583.

[18] K. Wade, *Adv. Inorg. Chem. Radiochem.* **1976**, *18*, 1.

[19] a) D. Seyferth, R. S. Henderson, *J. Am. Chem. Soc.* **1979**, *101*, 508; b) D. Seyferth, R. S. Henderson, M. K. Gallagher, *J. Organomet. Chem.* **1980**, *193*, C75; c) C. J. Cardin, D. J. Cardin, J. M. Power, *J. Am. Chem. Soc.* **1985**, *107*, 505; d) N. Viswanathan, E. Morrison, G. L. Geoffroy, S. J. Gib, A. L. Rheingold, *Inorg. Chem.* **1986**, *25*, 3100; e) R. D. Adams, D. A. Katahira, *Organometallics*, **1982**, *1*, 460.

[20] L. E. Bogan, Jr., T. B. Rauchfuss, A. L. Rheingold, *J. Am. Chem. Soc.* **1985**, *107*, 3843.

[21] D. A. Lesch, T. B. Rauchfuss, *Organometallics* **1982**, *1*, 1499.

[22] V. W. Day, D. A. Lesch, T. B. Rauchfuss, *J. Am. Chem. Soc.* **1982**, *104*, 1290.

[23] E. R. Brown, J. R. Sandifer in *Physical Methods of Chemistry. Electrochemical Methods*, *Vol. 2* (Eds.: B. W. Rossiter, J. F. Hamilton), Wiley, New York, **1986**, Chapter 4.

[24] R. G. Beevor, S. A. Genetti, *J. Organomet. Chem.* **1981**, *221*, C25.

[25] In analogy to the Me_5Cp derivative **4**.

[26] P. Zanello, F. Laschi, M. Fontani, C. Mealli, A. Ienco, K. Tang, X. Jin, L. Li, *J. Chem. Soc. Dalton Trans.* **1999**, in press.

Received: March 12, 1999 [F1670]

  0947-6539/00/0602-0246 $ 17.50+.50/0